Stereoselectivity of Each of the Three Steps of the Heme Oxygenase Reaction: Hemin to *meso*-Hydroxyhemin, *meso*-Hydroxyhemin to Verdoheme, and Verdoheme to Biliverdin†

Xuhong Zhang,‡ Hiroshi Fujii,*,§ Kathryn Mansfield Matera,||,⊥ Catharina Taiko Migita,||,# Danyu Sun,‡ Michihiko Sato,▽ Masao Ikeda-Saito,||,○ and Tadashi Yoshida*,‡

Department of Biochemistry and Central Laboratory for Research and Education, Yamagata University School of Medicine, Yamagata 990-9585, Japan, Institute for Molecular Science and Center for Integrative Bioscience, Okazaki National Research Institutes, Okazaki 444-8585, Japan, Department of Physiology and Biophysics, Case Western Reserve University School of Medicine, Cleveland, Ohio 44106-4970, and Institute of Multidisciplinary Research for Advanced Materials, Tohoku University, Sendai 980-8577, Japan

Received November 14, 2002; Revised Manuscript Received May 12, 2003

ABSTRACT: Heme oxygenase catalyzes the regiospecific oxidation of hemin to biliverdin IXα with concomitant liberation of CO and iron by three sequential monooxygenase reactions. The α-regioselectivity of heme oxygenase has been thought to result from the regioselective oxygenation of the heme α-*meso* position at the first step, which leads to the reaction pathway via *meso*-hydroxyheme IXα and verdoheme IXα intermediates. However, recent reports concerning heme oxygenase forming biliverdin isomers other than biliverdin IXα raise a question whether heme oxygenase can degrade *meso*-hydroxyhemin and isomers other than the α-isomers. In this paper, we investigated the stereoselectivity of each of the two reaction steps from *meso*-hydroxyhemin to verdoheme and verdoheme to biliverdin by using a truncated form of rat heme oxygenase-1 and the chemically synthesized four isomers of *meso*-hydroxyhemin and verdoheme. Heme oxygenase-1 converted all four isomers of *meso*-hydroxyhemin to the corresponding isomers of verdoheme. In contrast, only verdoheme IXα was converted to the corresponding biliverdin IXα. We conclude that the third step, but not the second, is stereoselective for the α-isomer substrate. The present findings on regioselectivities of the second and the third steps have been discussed on the basis of the oxygen activation mechanisms of these steps.

Microsomal heme oxygenase (HO)[1] catalyzes the conversion of hemin (ferric protoporphyrin IX) to biliverdin, CO, and free iron by using molecular oxygen and electrons donated by NADPH and NADPH−cytochrome P-450 reductase (reductase system) (*1*−*5*). The HO reaction consists of three sequential reactions (Scheme 1). In the first step, HO first binds the substrate hemin to form a hemin−enzyme complex (*6*, *7*). One electron donated from the reductase system reduces the ferric iron to the ferrous state (*8*), thus allowing molecular oxygen to bind to the ferrous iron to form a metastable oxy form (*9*, *10*). Further reduction and protonation convert the oxyheme to the hydroperoxyhemin, which has been recently established to be the active species of this step (*11*−*13*). The distal oxygen atom of the hydroperoxyhemin attacks its own α-*meso*-carbon to form *meso*-hydroxyhemin IXα. The second step is conversion of *meso*-hydroxyhemin to ferrous verdoheme using dioxygen and one electron (*14*−*17*). During this step, CO is liberated (*18*). The third step is the ring opening of verdoheme to the biliverdin−ferric iron complex using dioxygen and electrons (*19*, *20*). Although the last two steps require activated oxygen species, the mechanisms of the oxygen activation have not been established. Finally, biliverdin and ferrous iron are released from the enzyme, after reduction of the ferric iron of the complex (*8*), resulting in the completion of one cycle of the HO reaction. Therefore, in the HO reaction, hemin (*7*, *8*) and the two intermediates, *meso*-hydroxyhemin and verdoheme, serve both as substrates of the enzyme and as prosthetic groups for dioxygen activation. This feature gives HO a unique property not typically seen with most enzymes.

Formation of biliverdin from heme is stoichiometric (*21*) and only the IXα isomer is produced (*22*−*24*), demonstrating that the first step of the reaction is regiospecific. Yoshinaga

† This work was supported by grants-in-aid from the Ministry of Education, Science, Sports, and Culture, Japan (14340212, 12680549, 12147201, 14380300, 12680625, and 14580641), and by an NIH grant (GM57272).

* To whom correspondence should be addressed. T.Y.: phone, +81-23-628-5222; fax, +81-23-628-5225; e-mail, tyoshida@med.id.yamagata-u.ac.jp. H.F.: phone and fax, +81-564-55-7387; e-mail, hiro@ims.ac.jp.

‡ Department of Biochemistry, Yamagata University School of Medicine.

§ Institute for Molecular Science and Center for Integrative Bioscience, Okazaki National Research Institutes.

|| Department of Physiology and Biophysics, Case Western Reserve University School of Medicine.

⊥ Present address: Department of Chemistry, Baldwin-Wallace College, Berea, OH 44017.

Permanent address: Department of Biological Chemistry, Faculty of Agriculture, Yamaguchi University, Yamaguchi 753-8515, Japan.

▽ Central Laboratory for Research and Education, Yamagata University School of Medicine.

○ Institute of Multidisciplinary Research for Advanced Materials, Tohoku University.

[1] Abbreviation: HO, heme oxygenase.

10.1021/bi027173g CCC: $25.00
Published on Web 06/03/2003

Scheme 1: Heme Degradation Pathway by HO

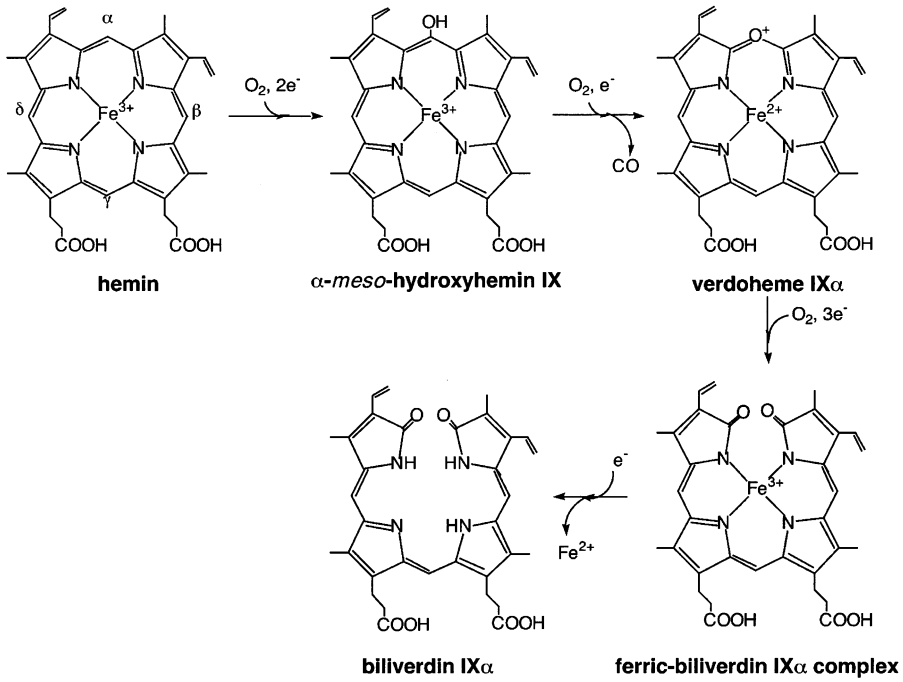

et al. (*17*) studied the reactivity of the four possible *meso*-hydroxyhemin isomers with HO and found that only the α-isomer was converted to the corresponding biliverdin IXα. However, the spectrophotometric properties of HO-1 complexed with the three isomers of *meso*-hydroxyhemin and of verdohemes other than the α-isomer and the mechanism of each step of the reactions from *meso*-hydroxyhemin and verdoheme have not been investigated.

Random cleavage of hemin at any one of the four structurally nonidentical *meso* positions, labeled α, *β*, *γ*, and *δ*, would yield the four corresponding isomers of biliverdin. Although hemin catabolism by HO-1 produces only the α-isomer (*22*−*24*), coupled oxidation of pyridine−hemin with ascorbic acid yields all four biliverdin isomers in nearly equal proportions, and biliverdin IX*δ* is formed when the highly conserved arginine-183 residue of rat HO-1 is mutated to acidic amino acid residues (*25*). Furthermore, PigA, a HO of *Pseudomonas aeruginosa*, has been reported to produce biliverdin IX*β* as a major product despite its significant amino acid sequence homology (37%) to HO of *Neisseria meningitides* (*26*), which exclusively forms biliverdin IXα (*27*). These findings indicate that α-specificity is not essential for HO reaction and raise questions about the stereoselectivity of each of the steps in the overall process. To address these questions, we prepared all four isomers of *meso*-hydroxyhemin and verdoheme and studied their conversion to the corresponding biliverdin when reconstituted into rat HO-1. We have found that the second step of the HO-1 reaction is nonselective for the isomeric *meso*-hydroxyhemin substrate, as reported previously (*17*), but the third step is selective for verdoheme IXα.

EXPERIMENTAL PROCEDURES

Materials. Soluble and catalytically active rat HO-1 30 kDa protein was prepared as described previously (*28*, *29*) and used without further purification. Not more than 10% was present as the biliverdin IXα complex, formed from catalytic degradation of bacterial (*Escherichia coli*) hemin. Rat NADPH−cytochrome P-450 reductase was a gift from Professor Bettie Sue Siler Masters (University of Texas Health Science Center at San Antonio). Each isomer of *meso*-benzoyloxyhemin was synthesized by the published method (*30*). Since the four isomers of *meso*-benzoyloxyporphyrin elute close to each other on silica gel chromatography, we were unable to isolate all four in pure form despite several-step purifications. ^{1}H NMR measurements of each fraction showed that the α- and *γ*-isomers of *meso*-benzoyloxyporphyrin were almost pure, but *β*- and *δ*-isomers contained a small amount of the *γ*-isomer (∼10%) and *β*-isomer (∼15%), respectively. Each isomer of *meso*-hydroxyhemin was prepared by the hydrolysis of the corresponding isomer of *meso*-benzoyloxyhemin under unaerobic conditions (*14*). Verdoheme IXα was synthesized from biliverdin IXα by the published method (*31*). *β*-, *γ*-, and *δ*-verdoheme isomers were synthesized by the air oxidation of the corresponding isomers of *meso*-hydroxyhemin in pyridine (*32*). Crude verdoheme complexes were purified by a preparative TLC (silica gel, 200 × 200 × 0.25 mm) with pyridine:chloroform:water = 6:4:1 by volume.

Optical absorption spectra were recorded on a Hewlett-Packard 8453 single-beam spectrophotometer at 20 °C throughout the present study. To analyze the isomers of biliverdin, an HPLC system (Jasco) equipped with a column of Capcell Pak C18 (SG 120, 4.6 × 150 mm, Shiseido) was used. The column was preequilibrated with degassed acetonitrile−water (3:2 v/v). The four isomers of biliverdin dimethyl ester were eluted with acetonitrile−water (3:2 v/v) at a flow rate of 1 mL/min in the order α, *δ*, *β*, and *γ*.

Preparation of Isomeric meso-Hydroxyhemin−*HO-1 Complexes.* For the reconstitution of the *meso*-hydroxyhemin−HO-1 complex, a HO-1 solution in 0.1 M potassium phosphate buffer (pH 7.0) was titrated with the *meso*-hydroxyhemin in 0.1 M NaOH solution under strict anaerobic conditions until 90% of the complex formed. The titrations

were done using a long-stem optical cuvette with a screw top fitted for a rubber septum for evacuation and introduction of gases, designed by Dr. H. Hori of Osaka University (Osaka, Japan). Prior to the titration, O_2 was removed by repeated evacuation followed by filling with nitrogen gas, and then the cuvette was filled with N_2 gas to 1.2 atm. Absorption spectra were recorded after each addition of a hemin solution.

Catabolic Reactions of Isomeric meso-Hydroxyhemin−HO-1 Complexes. The reaction mixture in a long-stem optical cuvette under strict anaerobic conditions contained, in a final volume of 2 mL, 0.1 M potassium phosphate buffer (pH 7.0), ~10 μM isomeric *meso*-hydroxyhemin−HO-1 complex, and 0.044 μM reductase. Reactions were initiated by the addition of 10 μL of 6 mM NADPH (final concentration of 30 μM) and exposing the reaction mixture to air. The optical spectra were measured with potassium phosphate buffer (pH 7.0) as reference.

Catabolic Reactions of Each Isomer of the Ferrous−CO Forms of meso-Hydroxyheme−HO-1 Complexes. The reaction mixture in a long-stem optical cuvette under CO contained, in a final volume of 2 mL, 0.1 M potassium phosphate buffer (pH 7.0) and ~6 μM isomeric *meso*-hydroxyhemin−HO-1 complex. After reduction of the *meso*-hydroxyhemin with a stoichiometric amount of sodium dithionite, the reaction was initiated by exposing the reaction mixture to air. The optical spectra were measured with potassium phosphate buffer (pH 7.0) as reference.

Preparation of Isomeric Verdoheme−HO-1 Complexes. For preparation of verdoheme−HO-1 complexes, HO-1 solution in CO-saturated 0.1 M potassium phosphate buffer (pH 7.0) was mixed with the verdoheme dissolved in a mixture (5% v/v) of pyridine and CO-saturated 0.1 M potassium phosphate buffer (pH 7.0). Excess verdoheme was removed on a column of Sephadex G-25 equilibrated with CO-saturated potassium phosphate buffer (pH 7.0). The CO complex was converted to the deoxy form by repeated evacuation followed by filling with nitrogen gas in the long-stem optical cuvette. Conversion was confirmed by recording the optical absorption spectrum.

Reactions of Isomeric Verdoheme−HO-1 Complexes. The reaction mixture in a long-stem optical cuvette under strict anaerobic conditions contained, in a final volume of 2 mL, 0.1 M potassium phosphate buffer (pH 7.0), ~20 μM isomeric verdoheme−HO-1 complex, and 0.044 μM reductase. Reactions were initiated by the addition of 10 μL of 6 mM NADPH (final concentration of 30 μM) and exposing the reaction mixture to air. Optical spectra were measured with potassium phosphate buffer (pH 7.0) as reference.

Isolation and Esterification of Biliverdin. The reaction mixture (1 mL) containing biliverdin was applied to a Supelclean LC-18 solid-phase extraction column (Supelco, Inc.) preconditioned with 400 μL of acetonitrile followed by 0.1 M Tris-HCl buffer (pH 7.4) containing 0.5 mg/mL bovine serum albumin. After the column was washed with 400 μL of acetonitrile−water (1:9 v/v), elution of a green pigment with 400 μL of acetonitrile−water (1:1 v/v) was carried out. The fractions containing the green pigment were collected and freeze-dried. Products were dissolved in 100 μL of 5% HCl−methanol and kept at 4 °C overnight. Biliverdin dimethyl ester was extracted into chloroform by treatment with 500 μL of chloroform−water (1:4 v/v). The chloroform layer was washed four times with 400 μL of water and then dried under a stream of argon gas. Dried materials were dissolved in 10 μL of chloroform, and then 2.5 μL of this sample was analyzed by HPLC to determine isomer composition.

RESULTS AND DISCUSSION

Properties of the Complexes of HO-1 with Four meso-Hydroxyhemin Isomers. As reported already (*14*), the absorption spectrum of the ferric α-*meso*-hydroxyheme−HO-1 complex has a broad Soret band with a featureless visible region (solid line in Figure 1A), whereas the deoxy (broken line) and the ferrous−CO forms (dotted line) have typical absorption spectra of heme proteins. The absorption spectra of the HO-1 complexes of the β-, γ-, and δ-isomers as well as the α-isomer are also shown in Figure 1, and the spectroscopic data are summarized in Table 1. The HO-1 complexed with the β-, γ-, and δ-isomers showed rather featureless visible region absorption spectra with broad Soret bands at 405, 413, and 405 nm, respectively (solid lines in Figure 1B−D). On the other hand, the deoxy forms of all four isomers (broken lines in Figure 1B−D) exhibited similar absorption spectra with Soret bands at 430 nm, whereas the spectra of the ferrous−CO forms of β-, γ-, and δ-isomers showed distinct but close bands at 421, 425, and 421 nm, respectively (dotted lines in Figure 1B−D). The spectral similarities of these isomers to those of the α-isomer indicate that the three isomers are properly incorporated in the heme pocket of HO-1, as previously supposed (*17*).

Reactivity of meso-Hydroxyhemin Isomer−HO-1 Complexes. We investigated the reactivity of each isomer of the four *meso*-hydroxyhemins. Figure 2 shows the absorption spectral change for each isomer of *meso*-hydroxyhemin bound to HO-1 before and 20 min after addition of the reductase system and air. As already reported, *meso*-hydroxyhemin IXα is converted to biliverdin IXα in the presence of reducing equivalents and oxygen (Figure 2A) (*14*, *15*, *17*). The spectral change shown in Figure 2A did not show clear isosbestic points due to formation of some intermediates in the reaction (data not shown). On the other hand, the reactions of the HO-1 complexes with the β-, γ-, and δ-isomers of *meso*-hydroxyhemin are different from that of the α-*meso*-hydroxyhemin−HO-1 complex. As the reaction proceeds, the Soret peaks of the other three isomers decrease in intensity, as observed for the *meso*-hydroxyhemin IXα complex, but the spectra of the final reaction products lack an absorption in the red region and resemble those of nonenzymatically decomposed heme (Figure 2B−D). These results confirm previous findings (*17*) that HO-1 does not degrade the β-, γ-, and δ-isomers of *meso*-hydroxyhemin to the corresponding biliverdin isomers with oxygen and reducing equivalents. Time course spectra of these reactions also did not exhibit clear isosbestic points during the reactions, thereby suggesting the presence of intermediate(s) in these nonenzymatic processes. The intermediate is possibly verdoheme because each isomer of *meso*-hydroxyhemin can be degraded to the corresponding verdoheme isomers by HO-1 as shown in the next section.

Reactivity of the CO-Bound Form of meso-Hydroxyheme Isomer−HO-1 Complexes and Substrate Selectivity of the Second Step of the Heme Oxygenase-1 Reaction from meso-

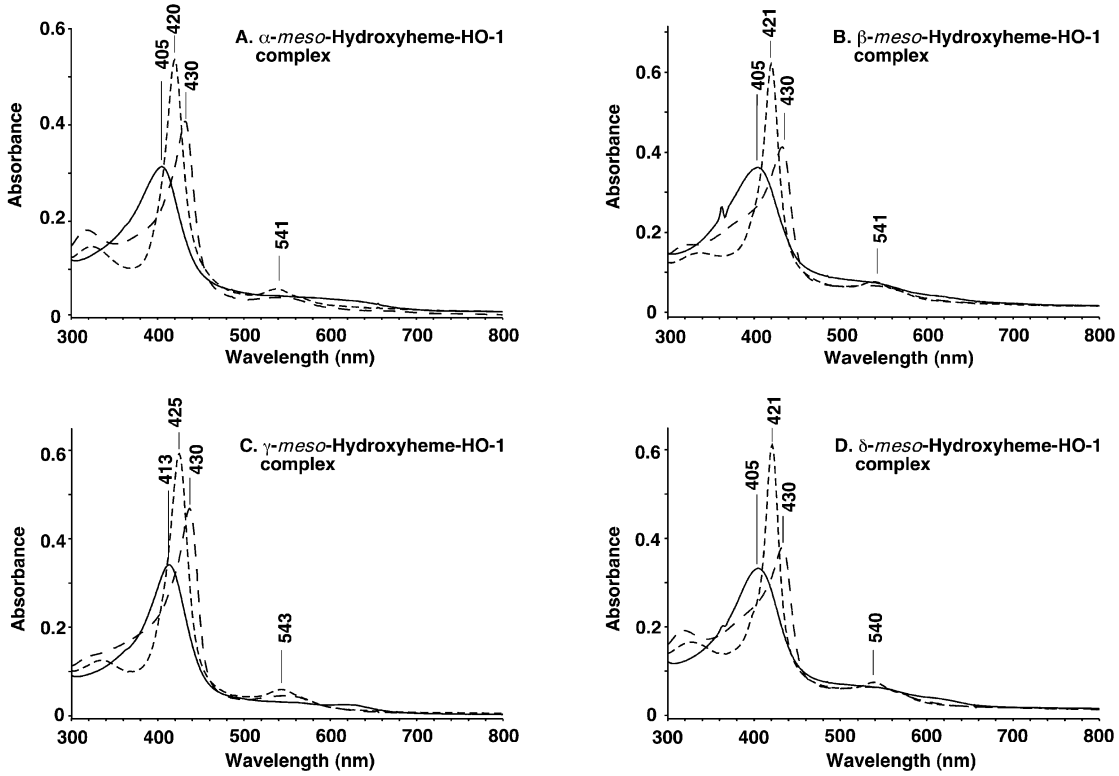

FIGURE 1: Optical absorption spectra of the isomeric *meso*-hydroxyheme−HO-1 complexes. Panels A−D represent *meso*-hydroxyhemin IXα, IX*β*, IX*γ*, and IX*δ*, respectively. Solid lines show absorption spectra of ferric forms, broken lines ferrous forms, and dotted lines ferrous CO-bound forms. In each case, the solution of 0.1 M potassium phosphate buffer (pH 7.0) contains ~4 *μ*M *meso*-hydroxyhemin isomer.

Table 1: Wavelengths of Absorption Maxima of Isomeric *meso*-Hydroxyheme−HO-1 Complexes

	λ_{max} (nm)		
	ferric	ferrous	ferrous−CO
α-isomer	405	430	420
			541
β-isomer	405	430	421
			541
γ-isomer	413	430	425
			543
δ-isomer	405	430	421
			540

Hydroxyhemin to Verdoheme. To further investigate the HO-1 reactions of *β*-, *γ*-, and *δ*-isomers of *meso*-hydroxyhemin, we carried out the HO-1 reaction of *meso*-hydroxyhemin to verdoheme. Previously, we observed that the CO-bound form of the α-*meso*-hydroxyheme−HO-1 complex was rapidly converted to the verdoheme complex after exposure to air (*14*) and that the reaction halted at this stage because CO arrested the further conversion of verdoheme to the biliverdin−iron complex (*18*). Therefore, we conducted similar experiments with the ferrous−CO forms of the isomeric *meso*-hydroxyhemin−HO-1 complexes. Figure 3 shows spectral changes for each isomer of the CO-bound form of the complexes after exposure to air. As observed for the α-isomer, the conversion of the other three isomers of *meso*-hydroxyhemin to verdoheme was not inhibited at all in the presence of CO. The absorption spectra of the respective ferrous−CO complexes of *meso*-hydroxyheme IX*β*, IX*δ*, and IX*γ* rapidly changed to those of the corresponding verdoheme isomers after exposure to air. In Table 2, the absorption maxima of these products are tabulated together with those of the four authentic verdoheme isomer−HO-1 complexes, whose optical spectra are shown in Figure 4. The good agreement of each λ_{max} value of the reaction product with that of the CO-bound form of the corresponding authentic verdoheme−HO-1 complex clearly indicates that all four *meso*-hydroxyheme isomers are converted to their respective verdoheme isomers by HO-1.

Table 2: Wavelengths of Absorption Maxima of Isomeric Verdoheme−HO-1 Complexes and of the Degradation Products from Isomeric *meso*-Hydroxyhemin−HO-1 Complexes under O_2 and CO

	λ_{max} (nm)		
	authentic verdoheme		products from *meso*-hydroxyhemin isomers
	ferrous	ferrous−CO	
α-isomer	399	408	405
	686	638	637
β-isomer	398	404	405
	669	623	623
γ-isomer	395	400	402
	655	615	617
δ-isomer	398	405	405
	665	624	622

Reactivity of Verdoheme Isomer−HO-1 Complexes and Substrate Selectivity of the Third Step of the HO-1 Reaction from Verdoheme to Biliverdin. To further study the substrate selectivity of each step of the HO-1 reaction, we examined the HO-1 reactions from each of the α-, *β*-, *γ*-, and *δ*-isomers of verdoheme to biliverdin. The absorption spectral features of the latter three verdoheme−HO-1 complexes are close to that of the α-verdoheme−HO-1 complex, but the peak positions are different in the four isomers (Figure 4, Table

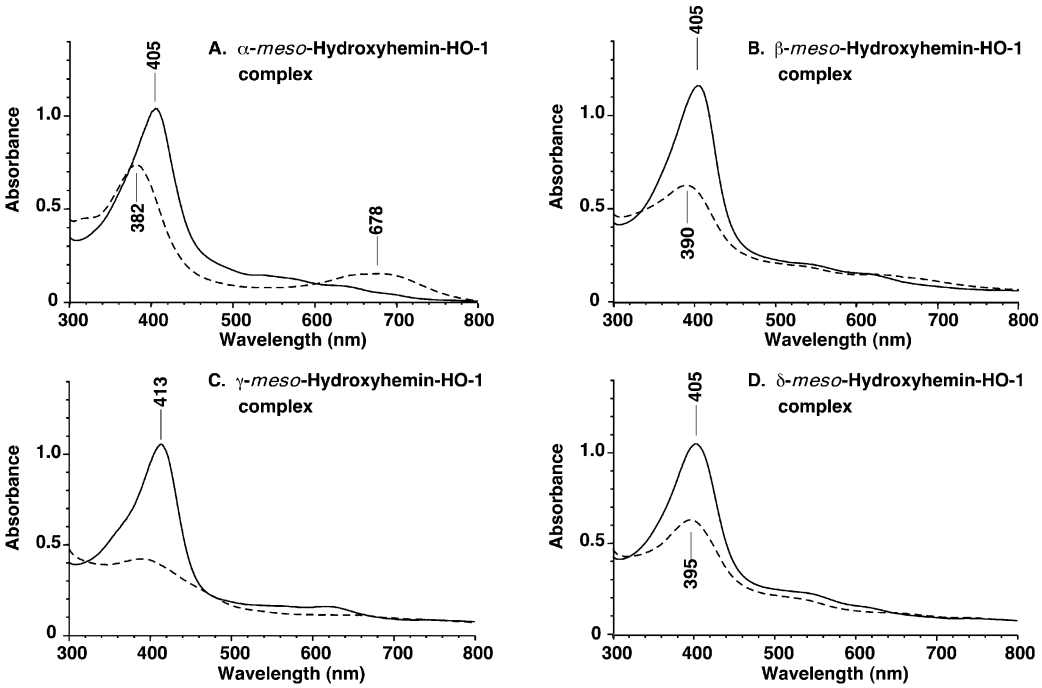

FIGURE 2: Catabolic reactions of the isomeric *meso*-hydroxyhemin−HO-1 complexes. Panels A−D correspond to the α-, *β*-, *γ*-, and *δ*-isomers, respectively. Solid lines show absorption spectra of each *meso*-hydroxyhemin isomer−HO-1 complex and broken lines absorption spectra of the reaction mixtures recorded 20 min after the start of the reaction. Reaction conditions are given in Experimental Procedures.

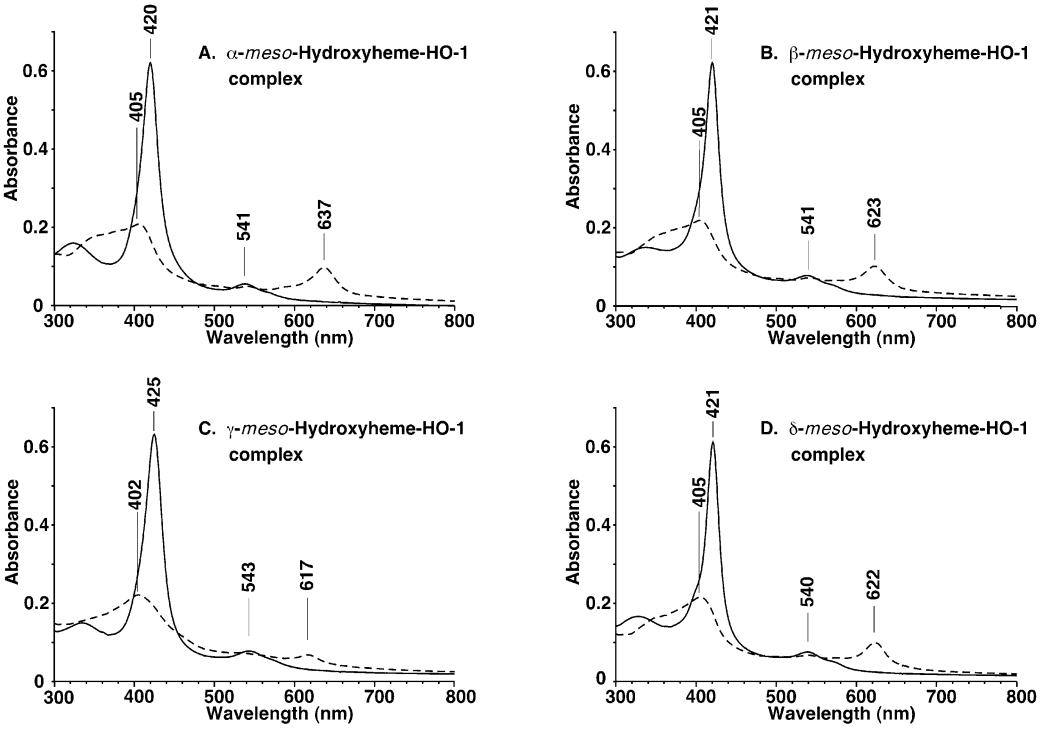

FIGURE 3: Conversion of isomeric ferrous−CO forms of the *meso*-hydroxyhemin complexes to their corresponding ferrous−CO forms of the verdoheme complexes upon exposure to air. Panels A−D correspond to the α-, *β*-, *γ*-, and *δ*-isomers, respectively. Solid lines show ferrous−CO forms of the *meso*-hydroxyhemin−HO-1 complex and broken lines those after 10 min after exposure to air. Reaction conditions are given in Experimental Procedures.

2). We added the reductase system to examine the spectral changes of the respective HO-1 complexes with verdoheme isomers. Solid and dotted lines in Figure 5 show the absorption spectrum before and after the reaction, respectively. In the case of the α-verdoheme−HO-1 complex, the absorption spectrum of the product exhibited the Soret band at 382 nm and a broad absorption peak around 670 nm, which is indicative of biliverdin formation. In the cases of the *β*-, *γ*-, and *δ*-verdoheme−HO-1 complexes, the absorption spectra of the reaction products also have significant absorption in the red region (Figure 5B−D), but the final spectrum of each isomer is different from that of the corresponding biliverdin isomer. These spectral data suggest that verdoheme IXα is enzymatically converted to biliverdin IXα by HO-1, while the other three isomers are not. This is further confirmed by HPLC analysis of the reaction products (Figure

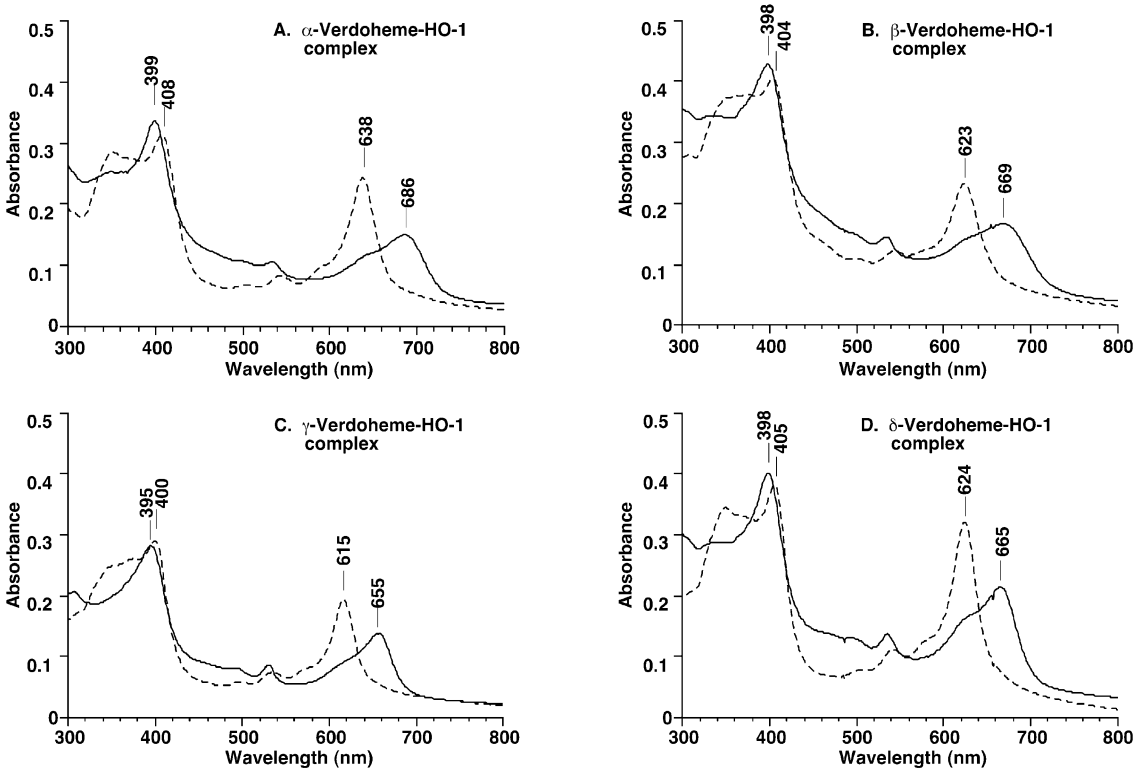

FIGURE 4: Absorption spectra of the isomeric verdoheme−HO-1 complexes. Panels A−D correspond to the α-, *β*-, *γ*-, and *δ*-isomers, respectively. Solid lines show ferrous forms and dotted lines ferrous CO-bound forms. The sample solutions contained final concentrations of ~15 *μ*M verdoheme isomers.

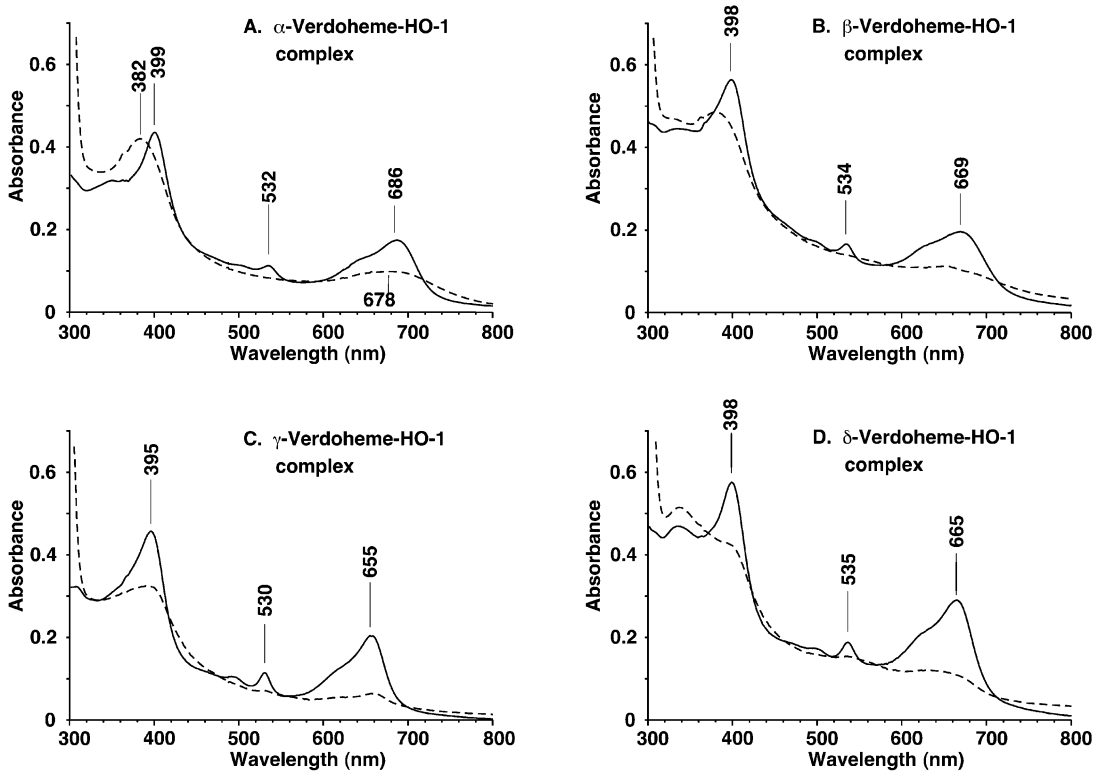

FIGURE 5: Catabolic reactions of the isomeric verdoheme−HO-1 complexes. Solid lines show optical absorption spectra of the isomeric verdoheme−HO-1 complexes and dotted lines those of the reaction products recorded 20 min after the start of the reaction. Reaction conditions are given in Experimental Procedures.

6). Figure 6A definitively shows that verdoheme IXα is degraded to biliverdin IXα stoichiometrically. On the other hand, the reaction products of verdoheme IX*β*, IX*γ*, and IX*δ* do not yield quantitative amounts of biliverdin isomers as shown by HPLC (Figure 6B−D). The small HPLC peaks corresponding to biliverdin IXα in Figure 6B−D result from endogenous biliverdin IXα bound to the purified HO-1 enzyme used in this work, whose concentration is determined

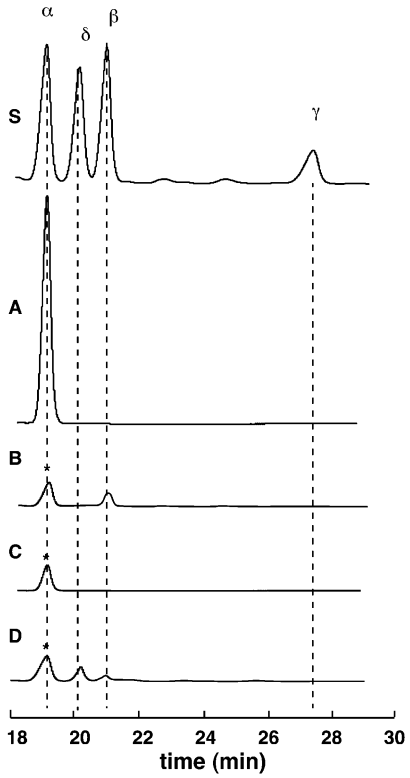

FIGURE 6: HPLC analysis of the products from the reaction of the four isomers of verdoheme−HO-1 complexes with the reductase system under air. The reaction conditions were similar to those described in Figure 5. The product analysis with HPLC was described in Experimental Procedures. Key: S, standard mixture of biliverdin IXα, IX*β*, IX*γ*, and IX*δ* dimethyl esters; A−D, products from verdoheme IXα, IX*β*, IX*γ*, and IX*δ*, respectively. The peaks marked by an asterisk at the position of biliverdin IXα in panels B−D are due to endogenous biliverdin IXα bound to the enzyme.

to be less than 10% from the absorption peak intensity at 657 nm. The bound biliverdin IXα is derived from catalytic degradation of bacterial (*E. coli*) hemin, which could not be removed from the enzyme in the course of purification. Since the peak intensity of the α-isomer in Figure 6B−D indicates less than 10% yield, the small peak of biliverdin IX*β* from verdoheme IX*β* (in Figure 6B) and those of biliverdins IX*β* and IX*δ* from verdoheme IX*δ* (in Figure 6D) are estimated to be less than 5% yield. These trace amounts of biliverdin isomers may be produced by acid hydrolysis of unreacted verdoheme in the reaction solution. The HPLC peak of biliverdin IX*β* in Figure 6D is due to contamination of the *β*-isomer into the *δ*-isomer during its preparation. Since verdoheme IX*δ* is synthesized from *meso*-hydroxyheme IX*δ*, the verdoheme IX*δ* sample also contains ∼15% of verdoheme IX*β* (cf. Experimental Procedures). Accordingly, these results suggest that the *β*-, *γ*-, and *δ*-isomers of verdoheme are not enzymatically converted to the corresponding biliverdin isomers by the HO-1. All of these findings establish that the third step of the HO-1 reaction is selective for verdoheme IXα.

Stereoselectivity of the HO-1 Reaction. In the first step, the α-bridge carbon of hemin is oxidized regiospecifically by the hydroperoxy group of the hemin intermediate, the active species of this step. The hemin−HO-1 complex has the distal helix within 4 Å across the entire width of the heme, which sterically prevents access of the iron-bound hydroperoxy species to the *β*-, *γ*-, and *δ*-*meso*-carbon atoms (*33*). Furthermore, the hydrogen bond of the iron-bound hydroperoxy species with the aspartate-140 residue of rat HO-1 through a water molecule would direct the terminal oxygen of the hydroperoxy species to the α-*meso* carbon (*34*). Thus, the iron-bound hydroperoxy species can oxygenate only the α-*meso* carbon of hemin, resulting in the α-regioselectivity of the first step. In contrast to the first step of the HO reaction, oxygen activation on heme iron is not involved in the second step. As suggested by previous studies (*32*, *35*), molecular oxygen reacts directly with the activated carbon adjacent to the hydroxylated *meso*-carbon, without the participation of heme iron. Thus, the steric and hydrogen-bonding effects of the distal helix are unimportant, and all four isomers are converted to the corresponding verdoheme complexes.

Although the mechanism of the third step has not been elucidated, an active oxygen species such as superoxide or a hydroperoxy species seems to be formed on the verdoheme iron. This is because CO (*18*) and cyanide (*19*) bound to the iron of verdoheme inhibit this third step. Possibly, as proposed for the first step, the active oxygen species formed on the verdoheme iron can oxygenate only the α-*meso*-carbon bridge of verdoheme due to the steric and hydrogen-bonding effects of the distal helix. Yoshinaga et al. (*17*) reported that the *β*-, *γ*-, and *δ*-isomers of *meso*-hydroxyhemin can bind to the active site of HO at the same position as the α-hydroxyhemin isomer on the basis of the competitive inhibition of biliverdin IXα formation from α-*meso*-hydroxyhemin IX by *β*-, *γ*-, or *δ*-isomers of *meso*-hydroxyhemin. Likely, this is the case for the binding of isomers of verdoheme. In addition, we observed that CO (Supporting Information, Figure S-1) and cyanide (Supporting Information, Figure S-2) inhibited not only the conversion of verdoheme IXα to biliverdin IXα but also the decomposition of the *β*-, *γ*-, and *δ*-isomers of verdoheme to non-biliverdin products. Taken together, we suppose that each of the verdoheme isomers bound to HO-1 except the α-isomer was attacked by activated oxygen at the innermost *meso* bridge rather than the oxo bridge, resulting in the formation of non-biliverdin products.

Physiological Significance of α*-Specificity of the HO Reaction.* In some nonmammalian vertebrates biliverdin IXα produced by the HO reaction is the final product excreted in bile (*36*). In mammals, biliverdin is reduced to bilirubin by biliverdin reductase at the expense of NADPH. Two enzymes, α-reductase (*37*, *38*) and *β*-reductase (*39*, *40*), have been reported. α-Reductase uses only biliverdin IXα as the natural substrate, whereas *β*-reductase uses biliverdins IX*β*, IX*γ*, and IX*δ* as a substrate but not biliverdin IXα. However, the isomeric composition of the pigments in bile in mammals is virtually all the IXα type with minor traces of the *β*- and *δ*-isomers of bilirubin (*41*), reflecting that physiological heme catabolism is mediated principally by HO.

Of the four isomers of bilirubin, only bilirubin IXα is lipophilic, because its propionic acid side chains are involved in the formation of intramolecular hydrogen bonding. In contrast, the three other isomers are relatively polar. Since neither biliverdin nor, probably, bilirubin IX*β*, IX*γ*, and IX*δ* cross the placenta as readily as lipophilic bilirubin IXα (*42*), reduction of biliverdin IXα to bilirubin IXα is indispensable to mammals. If a mammal were to produce only the *β*-, *γ*-,

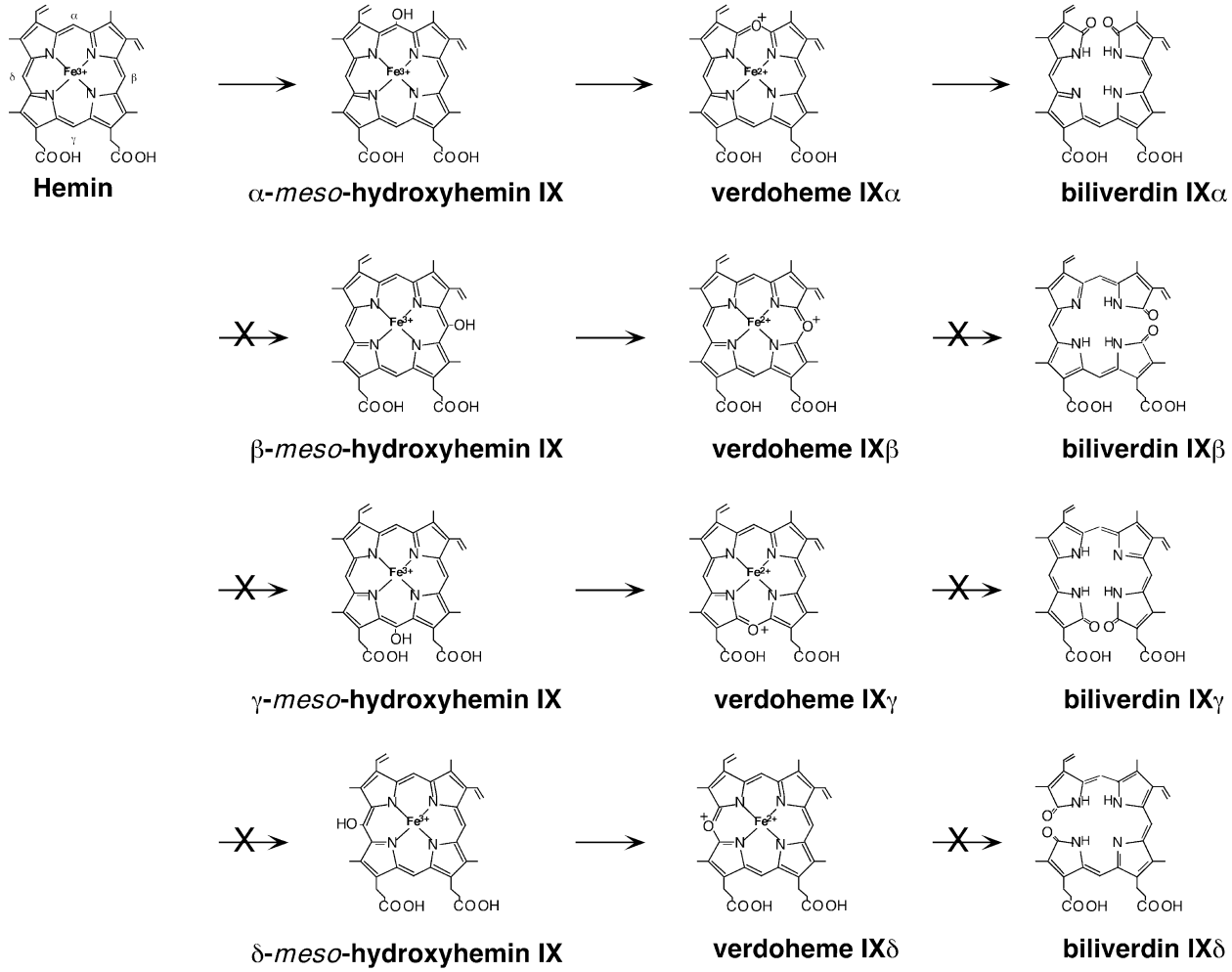

FIGURE 7: Stereoselectivity in the HO-1 reaction summarized from the results of the present and previous studies.

and δ-isomers, these would, presumably, accumulate and be toxic to the fetus. This explains why α-selectivity of heme degradation, i.e., the selective biliverdin IXα formation, is important in mammals. In addition, bilirubin IXα is now widely accepted to be a potent endogenous lipid-soluble antioxidant, which acts as a breaker of chain oxidation of unsaturated fatty acids in membranes with a potency similar to that of α-tocopherol (*43*, *44*).

CONCLUSIONS

Figure 7 shows the overall stereoselectivity of the HO reaction based on the present and preceding works. In the first step of the HO reaction, it is accepted that hydroperoxo species bound to heme iron can react only with the α-*meso* carbon of hemin because of protein steric control, resulting in α-specificity. The second step is not selective for a particular isomer of *meso*-hydroxyhemin, probably because this step does not involve activation of oxygen by the ferrous−heme iron. The third step is revealed to be stereoselective for the α-isomer of verdoheme. We infer that, in the third step, the iron of ferrous verdoheme participates in oxygen activation and that, by analogy to the first step, the active oxygen species on verdoheme iron is sterically restricted to attack the α-position.

SUPPORTING INFORMATION AVAILABLE

Figure S-1 showing that CO inhibited significantly degradation of the four isomers of verdoheme and Figure S-2 showing that cyanide inhibited drastically degradation of the four isomers of verdoheme. This material is available free of charge via the Internet at http://pubs.acs.org.

REFERENCES

1. Tenhunen, R., Marver, H. S., and Schmid, R. (1969) *J. Biol. Chem. 244*, 6388−6394.
2. Maines, M. D. (1988) *FASEB J. 2*, 2557−2568.
3. Sono, M., Roach, M. P., Coulter, E. D., and Dawson, J. M. (1996) *Chem. Rev. 96*, 2841−2887.
4. Ortiz de Montellano, P. R. (1998) *Acc. Chem. Res. 31*, 543−549.
5. Yoshida, T., and Migita, C. T. (2000) *J. Inorg. Biochem. 82*, 33−41.
6. Yoshida, T., and Kikuchi, G. (1978) *J. Biol. Chem. 253*, 4224−4229.
7. Yoshida, T., and Kikuchi, G. (1979) *J. Biol. Chem. 254*, 4487−4491.
8. Yoshida, T., and Kikuchi, G. (1978) *J. Biol. Chem. 253*, 4230−4236.
9. Yoshida, T., Noguchi, M., and Kikuchi, G. (1980) *J. Biol. Chem. 255*, 4418−4420.
10. Yoshida, T., Noguchi, M., and Kikuchi, G. (1980) *FEBS Lett. 115*, 278−280.
11. Davydov, R. M., Yoshida, T., Ikeda-Saito, M., and Hoffman, B. M. (1999) *J. Am. Chem. Soc. 121*, 10656−10657.

12. Davydov, R. M., Kofman, V., Fujii, H., Yoshida, T., Ikeda-Saito, M., and Hoffman, B. M. (2002) *J. Am. Chem. Soc. 124*, 1798−1808.
13. Denisov, I. G., Ikeda-Saito, M., Yoshida, T., and Sligar, S. G. (2002) *FEBS Lett. 532*, 203−206.
14. Mansfield Matera, K., Takahashi, S., Fujii, H., Zhou, H., Ishikawa, K., Yoshimura, T., Rousseau, D. L., Yoshida, T., and Ikeda-Saito, M. (1996) *J. Biol. Chem. 271*, 6618−6624.
15. Migita, C. T., Fujii, H., Mansfield Matera, K., Takahashi, S., Zhou, H., and Yoshida, T. (1999) *Biochim. Biophys. Acta 1432*, 203−213.
16. Liu, Y., Moenne-Loccoz, P., Loehr, T. M., and Ortiz de Montellano, P. R. (1997) *J. Biol. Chem. 272*, 6909−6917.
17. Yoshinaga, T., Sudo, Y., and Sano, S. (1990) *Biochem. J. 270*, 659−664.
18. Yoshida, T., Noguchi, M., and Kikuchi, G. (1982) *J. Biol. Chem. 257*, 9345−9348.
19. Yoshida, T., and Noguchi, M. (1984) *J. Biochem. (Tokyo) 96*, 563−570.
20. Wilks, A., and Ortiz de Montellano, P. R. (1993) *J. Biol. Chem. 268*, 22357−22362.
21. Noguchi, M., Yoshida, T., and Kikuchi, G. (1983) *J. Biochem. (Tokyo) 93*, 1027−1036.
22. Noguchi, M., Yoshida, T., and Kikuchi, G. (1982) *J. Biochem. (Tokyo) 91*, 1479−1483.
23. Docherty, J. C., Masters, B. S. S., Firneisz, G. D., and Schacter, B. R. (1982) *Biochem. Biophys. Res. Commun. 105*, 1005−1013.
24. Yoshinaga, T., Sassa, S., and Kappas, A. (1982) *J. Biol. Chem. 257*, 7794−7802.
25. Zhou, H., Migita, C. T., Sato, M., Sun, D., Zhang, X., Ikeda-Saito, M., Fujii, H., and Yoshida, T. (2000) *J. Am. Chem. Soc. 122*, 8311−8312.
26. Ratliff, M., Zhu, W., Deshmukh, R., Wilks, A., and Stojilikovic, I. (2001) *J. Bacteriol. 183*, 6394−6403.
27. Zhu, W., Wilks, A., and Stojilikovic, I. (2000) *J. Bacteriol. 182*, 6783−6790.
28. Ito-Maki, M., Ishikawa, K., Mansfield Matera, K., Sato, M., Ikeda-Saito, M., and Yoshida, T. (1995) *Arch. Biochem. Biophys. 317*, 253−258.
29. Mansfield Matera, K., Zhou, H., Migita, C. T., Hobert, S. E., Ishikawa, K., Katakura, K., Maeshima, H., Yoshida, T., and Ikeda-Saito, M. (1997) *Biochemistry 36*, 4909−4915.
30. Sano, S., Sano, T., Morishima, I., Shiro, Y., and Maeda, Y. (1986) *Proc. Natl. Acad. Sci. U.S.A. 83*, 531−535.
31. Saito, S., and Itano, H. A. (1986) *J. Chem. Soc., Perkin Trans. 1*, 1−7.
32. Morishima, I., Fujii, H., Shiro, Y., and Sano, S. (1995) *Inorg. Chem. 34*, 1528−1535.
33. Schuller, D. J., Wilks, A., Ortiz de Montellano, P. R., and Poulos, T. L. (1999) *Nat. Struct. Biol. 6*, 860−867.
34. Fujii, H., Zhang, X., Tomita, T., Ikeda-Saito, M., and Yoshida, T. (2001) *J. Am. Chem. Soc. 123*, 6475−6484.
35. Balch, A. L., Koerner, R., Latos-Gazynski, L., and Noil, B. (1996) *J. Am. Chem. Soc. 118*, 2760−2761.
36. O'Carra, P. (1975) in *Porphyrins and Metalloporphyrins* (Smith, K. M., Ed.) pp 123−153, Elsevier, Amsterdam.
37. Fakhrai, H., and Maines, M. D. (1992) *J. Biol. Chem. 267*, 4023−4029.
38. Kikuchi, A., Park, S. A., Miyatake, D., Sun, D., Sato, M., Yoshida, T., and Shiro, Y. (2001) *Nat. Struct. Biol. 8*, 221−225.
39. Yamaguchi, T., Komada, Y., and Nakajima, H. (1994) *J. Biol. Chem. 269*, 24343−24348.
40. Pereira, P. J. B., Macedo-Ribeiro, S., Parrage, A., Perez-Luque, R., Cunningham, O., Darcy, K., Mantle, T. J., and Coll, M. (2001) *Nat. Struct. Biol. 8*, 215−220.
41. O'Carra, P., and Colleran, E. (1970) *J. Chromatogr. 50*, 458−468.
42. McDonagh, A. F., Palma, N. A., and Schmid, R. (1981) *Biochem. J. 194*, 273−282.
43. Stocker, R., Yamamoto, Y., McDonagh, A. F., Glazer, A. N., and Ames, B. N. (1987) *Science 235*, 1043−1046.
44. Baranano, D. E., Rao, M., Ferris, C. D., and Snyder, S. H. (2002) *Proc. Natl. Acad. Sci. U.S.A. 99*, 16093−16098.

BI027173G